

Capillary Liquid Chromatography at Ultrahigh Pressures

James W. Jorgenson

Department of Chemistry, University of North Carolina at Chapel Hill, Chapel Hill, North Carolina 27599-3290; email: jj@unc.edu

Annu. Rev. Anal. Chem. 2010. 3:129–50

First published online as a Review in Advance on February 16, 2010

The *Annual Review of Analytical Chemistry* is online at anchem.annualreviews.org

This article's doi:
10.1146/annurev.anchem.1.031207.113014

Copyright © 2010 by Annual Reviews.
All rights reserved

1936-1327/10/0719-0129\$20.00

Key Words

UHPLC, high-resolution liquid chromatography, 1- μ m particles

Abstract

Ultrahigh-pressure liquid chromatography (UHPLC) is a method of liquid chromatography utilizing sub-2- μ m particles packed into capillary columns 25 to 100 cm long. Columns of this length packed with particles this fine require operation with pressures from 1,000 to 7,000 bar (15,000 to 100,000 psi). The advantages of this technique are high separation powers (theoretical plate counts from 100,000 to 300,000) and run times from a few minutes (isocratic) to a few hours (long gradients). This review discusses the background and theoretical basis of UHPLC, practical aspects of UHPLC hardware, examples of separations, future areas for research in UHPLC, and techniques that are both competitive with and complementary to UHPLC.

1. INTRODUCTION

The history of liquid chromatography (LC) is tied to the development of ever smaller particles for use as packing materials. Early chromatographic theory was developed in parallel with advances in gas chromatography (GC) in the 1950s and 1960s. This theory clarified the advantages of small particles in chromatography, principally reductions in two terms, eddy diffusion (A term) and resistance to mass transfer (C term), of the van Deemter equation. The theory predicted that the use of smaller and more uniform particles would result in more effective separations and faster optimum mobile-phase velocities—the irresistible pull of “better and faster.” The theory made no distinction between gases and liquids as the mobile phase; both GC and LC benefit from the use of smaller particles. Due to lower diffusivities in liquids as well as their relative incompressibility, the advantages of small particles proved to be greater in LC than in GC. The cost of using smaller particles in LC was a significant increase in operating pressure. Recall that the HP in the acronym HPLC stood for high pressure before it stood for high performance.

The transition from simple gravity-driven columns packed with large particles to sophisticated HPLC systems represented an entirely new approach to LC. Not only did these systems become faster and more effective at separation, they were automated; updated components included autosamplers, high-pressure/high-precision constant-flow pumps, small-particle columns, and online detectors with computer-based data acquisition. Following the introduction of HPLC, LC became an instrumental technique, boasting new levels of automation, accuracy, and precision and greatly improved detection limits, in addition to expected improvements in speed and resolution.

The equipment introduced early in the history of HPLC operated within a pressure limit of approximately 400 bar (6000 psi), a pressure that anticipated the operation of columns 25 cm long packed with particles as small as 5 μm . The 400-bar pressure limit provided plenty of leeway for operating these columns, allowing for increasing back pressure as the columns became plugged with use. This pressure limit was reflected in all components of the equipment—not only the pumps but also the column hardware, fittings, and valves. A small number of commercial systems operated at pressures of up to 550 bar, but no significant use was made of this modest increase in pressure capability.

The 400-bar pressure limit has remained in place for the past 35 years. Its selection was based on good principles involving heat generation and dissipation (1, 2). Indeed, in 1975 Halász et al. (1) proposed a 500-bar limit for HPLC on the basis of the following considerations. Due to viscous dissipation, heat is generated in the process of pumping mobile phase through a chromatography column. The rate of heat generation (power) is equal to the product of the pressure drop over the length of the column and the mobile-phase flow rate. Heat thus builds up in the mobile phase as it flows down the column. Heat is removed from the column in two ways. First, it simply flows along with the mobile phase and exits from the column outlet. Second, it dissipates through the walls of the column to the surroundings. These two mechanisms result in two temperature gradients: a temperature rise along the length of the column, from inlet to outlet, and a radial temperature gradient that has a warmer region on the column axis and that becomes progressively cooler toward the column wall. Both temperature gradients are potentially detrimental to column efficiency, but the radial gradient contributes more toward band spreading. The warmer fluid in the center of the column is less viscous and thus flows faster, resulting in band dispersion. Analyte distribution between the mobile and stationary phases is also temperature dependent; there is less retention in the warmer core region of the column, leading to increased band dispersion. Both of these effects work in the same direction, leading to faster elution of analytes in the warmer core of the column than in the cooler regions near the wall. Given this issue of heat generation and dissipation, and

Table 1 Trends in particle sizes, column dimensions, and performance in high-pressure liquid chromatography

Packing material	Column length (cm)	Pressure (bar)	Void time (min)	Column efficiency (plates)
10 μm , porous, irregular	25	16	2.5	7,000
5 μm , porous	25	66	2.5	20,000
3 μm , porous	10	122	0.6	13,000
2 μm , porous	5	206	0.2	10,000
1.5 μm , nonporous	3	263	0.1	8,000

given the 4.6-mm-bore column technology, 400 bar was a logical pressure limit. Although there were a few investigations of the effects of ultrahigh pressure on analyte retention and modifying selectivity in LC (3–6), there were no experiments on the use of ultrahigh pressures for pumping mobile phases through long columns packed with small particles.

Historical trends in the use of smaller particles in HPLC are summarized in **Table 1**. The development of packings below 5 μm required use of shorter columns in order to avoid approaching the 400-bar pressure limit. Shorter columns resulted in faster analysis times but also in a decrease in overall column-separation efficiency. By the year 2000, the highest separation efficiencies in conventional commercial HPLC columns were obtained with 5- μm particles packed in 25-cm-long columns; this technology was first introduced in the late 1970s.

In 1994 my laboratory began a research project to investigate the possibilities for sub-2- μm packing materials packed into long capillary columns and operated at ultrahigh pressures (7). The use of capillary columns in lieu of conventional column diameters results in significantly increased efficiency of radial heat dissipation and thus permits operation at pressures far in excess of the 400-bar limit of HPLC. **Table 2** summarizes the effects of column diameter on total heat generation. In all cases, the 50-cm-long columns are assumed to be packed with 1- μm particles and operated at a pressure of 7000 bar. In the case of a 4.6-mm-bore column, the rate of heat generation is 24 W (344 calories min^{-1}). Given a mobile-phase flow rate of 2 ml min^{-1} , the heat deposition is 172 calories ml^{-1} of effluent from the column. Assuming that radial heat dissipation from the column wall to the surroundings is a minor mode of heat dissipation in a column of this diameter, there is more than enough heat generated per milliliter of mobile phase to take the solvent from room temperature to the boiling point prior to elution from the column. This is too great a thermal load for a conventional-bore column to be operated with this pressure drop and flow rate.

Table 2 Heat generation in ultrahigh-pressure liquid chromatography^a

Column inner diameter	Flow rate	Pressure	Power
4.6 mm	2.0 ml min^{-1}	7000 bar	24.0 W
2.0 mm	380 $\mu\text{l min}^{-1}$	7000 bar	4.5 W
1.0 mm	95 $\mu\text{l min}^{-1}$	7000 bar	1.1 W
500 μm	24 $\mu\text{l min}^{-1}$	7000 bar	280 mW
250 μm	5.9 $\mu\text{l min}^{-1}$	7000 bar	71 mW
100 μm	940 nL min^{-1}	7000 bar	11 mW
50 μm	240 nL min^{-1}	7000 bar	2.9 mW

^aPower equals heat divided by time, which equals flow rate times pressure drop. Assume 1.0- μm particles packed in a 50-cm-long column.

^b24 W equals 344 calories min^{-1} or 172 calories ml^{-1} .

At the opposite extreme, for a 50- μm -bore column, the heat dissipation is approximately 3 mW. Experience with thermal loads in capillary electrophoresis, where heat dissipations of hundreds of milliwatts are acceptable for 50-cm-long capillaries, shows that this heat load is negligible and that no measurable effect of heating would be observed. For this flow rate and pressure drop, a column diameter of less than 500 μm would probably be required in order to avoid excess band spreading from thermal causes. Thus, LC at exceptionally high pressures must be performed in columns of capillary dimensions. We term this format ultrahigh-pressure LC (UHPLC).

2. THEORETICAL BASIS FOR ULTRAHIGH-PRESSURE LIQUID CHROMATOGRAPHY

Figure 1 shows the van Deemter curves that would be expected for packing materials measuring 5, 3, and 1 μm in diameter. The advantages of 1- μm particles are obvious: The plate-height minimum is proportional to the particle diameter, and the optimum mobile-phase velocity is proportional to the inverse of the particle diameter. By decreasing the particle diameter fivefold from 5 to 1 μm while maintaining the column length, one should observe the column efficiency increase fivefold and the time of analysis decrease fivefold. The cost of these improvements is pressure. As shown in **Table 1**, 5- μm particles packed into a 25-cm-long column should produce 20,000 theoretical plates with a column void time of 2.5 min and should require 66 bar of pressure to do so. From this starting point we can project that 1- μm particles packed into a 25-cm-long column should produce 100,000 theoretical plates (a fivefold increase) with a column void time of 30 s (fivefold faster) but that this process would require a 125-fold-greater pressure of 8000 bar. Use of micrometer-sized particles in long columns to achieve very high separation efficiencies with fast analysis times requires a huge increase in available pressure.

Consider the following question: If available pressure and available analysis time are limited (i.e., if we are not willing to consider unlimited pressure or analysis time), then are there an optimum particle size and column length to use in order to achieve the maximum separation

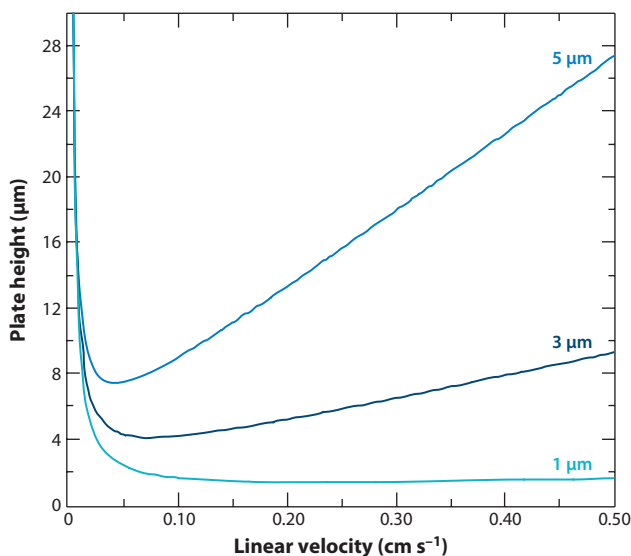


Figure 1

Hypothetical van Deemter curves for 5-, 3-, and 1- μm particles (13).

efficiency? The interstitial mobile-phase velocity (the average velocity of mobile phase flowing between the particles of packing material), u , is given in Equation 1, where P is the pressure dropped over the column length, d_p is the average particle diameter, ε is the interparticle volume fraction of the mobile phase (the fraction of total column volume between the particles), η is the mobile-phase viscosity, and L is the column length. Because ε is approximately 0.4 for a bed of random-packed spheres, Equation 1 can be simplified to the expression on the right-hand side of Equation 1:

$$u = \frac{Pd_p^2\varepsilon^2}{180\eta L(1-\varepsilon)^2} = \frac{Pd_p^2}{400\eta L}. \quad (1)$$

The void time (or dead time) of the column, t_m , is given in Equation 2. This is the time it would take for an unretained macromolecular marker that is excluded from any pores in the packing material to elute from the column. Equation 2 shows that if the pressure and void time are fixed at a maximum allowable value, then the column length and particle diameter of the packing material are dependent variables:

$$t_m = \frac{L}{u} = \frac{400\eta L^2}{Pd_p^2}. \quad (2)$$

Equations 3 and 4 are rearrangements of Equation 2. They show that column length is dictated by a choice of particle diameter and, conversely, that particle diameter is dictated by a choice of column length:

$$L = \left[\frac{Pt_m}{400\eta} \right]^{1/2} d_p \quad \text{and} \quad (3)$$

$$d_p = \left[\frac{400\eta}{Pt_m} \right]^{1/2} L. \quad (4)$$

Equation 5 is an approximate form of the van Deemter equation, one that we empirically find approximately correct for packed capillary columns. The height equivalent of a theoretical plate, H , is given by three terms on the right-hand side of the equation: (a) eddy diffusion, (b) longitudinal diffusion in the mobile phase, and (c) resistance to mass transfer in the mobile phase. D_m is the diffusion coefficient of the analyte in the mobile phase:

$$H = \frac{d_p}{2} + \frac{2D_m}{u} + \frac{d_p^2 u}{5D_m}. \quad (5)$$

In Equation 6, the mobile-phase velocity given in Equation 5 is substituted with the expression for mobile-phase velocity from Equation 1:

$$H = \frac{d_p}{2} + \frac{800\eta D_m L}{Pd_p^2} + \frac{Pd_p^4}{2000\eta D_m L}. \quad (6)$$

What we wish to do is maximize the number of theoretical plates, N , which is the quantitative descriptor of the column's separation efficiency. Equation 7 gives the number of theoretical plates, which is the ratio of the column length to the height equivalent of a theoretical plate. By substituting the expression for H given in Equation 6 into Equation 7, we find the expression for N on the right-hand side of Equation 7:

$$N = \frac{L}{H} = \frac{2000\eta D_m PL^2 d_p^2}{1000\eta D_m PL d_p^3 + (1.6 \times 10^6)\eta^2 D_m^2 L^2 + Pd_p^6}. \quad (7)$$

Now we substitute the expression for column length, L , given in Equation 3 into Equation 7 to obtain Equation 8, which describes the number of theoretical plates in terms of the

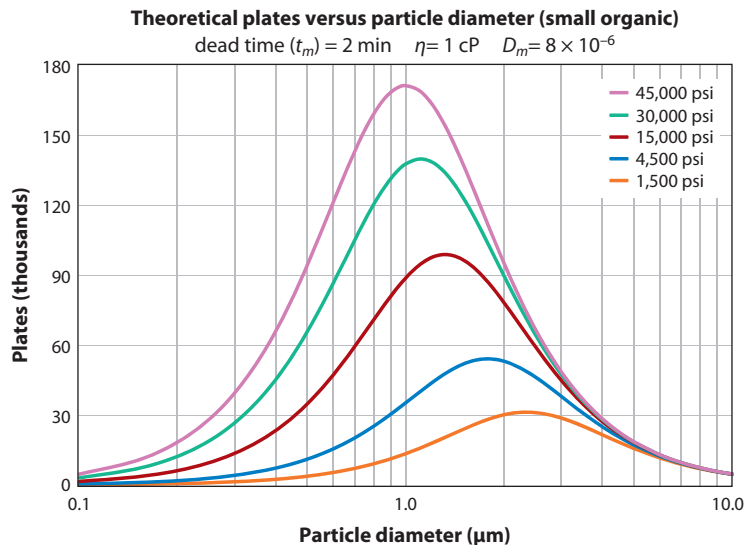


Figure 2

Hypothetical plots of separation efficiency as a function of particle diameter for columns operated at a series of pressures.

packing-material particle diameter as well as the few physical parameters of the column, namely pressure, void time, analyte diffusion coefficient, and mobile-phase viscosity:

$$N = \frac{5 D_m P d_p^2 t_m}{50 \eta^{1/2} D_m P^{1/2} d_p^2 t_m^{1/2} + 4000 \eta D_m^2 t_m + P d_p^4} \quad (8)$$

The resulting equation is complex, and its predictions are better appreciated in terms of graphs of column efficiency as a function of particle diameter, as shown in **Figure 2**. In this figure there is a family of curves, each corresponding to a different pressure, describing column efficiency as a function of particle diameter. For an applied pressure of 100 bar, which is typical for HPLC, Equation 8 predicts (a) an optimum particle diameter of approximately 2.5 μm , (b) a corresponding optimum column length of 13 cm, and (c) that such a column could provide as many as 30,000 theoretical plates. As the available pressure in this hypothetical column is increased, the optimum particle diameter decreases, and the optimum column length increases. At an applied pressure of 3000 bar, the optimum particle diameter is 1 μm , the corresponding optimum column length is 30 cm, and the efficiency is 170,000 plates. The maxima in these curves are a result of the interplay of longitudinal diffusion and resistance to mass transfer, the two terms in the van Deemter equation that give rise to the minima in van Deemter curves. For a given pressure and void time, a particle diameter smaller than the optimum dictates a shorter column length (Equation 3), resulting in excessive band spreading due to longitudinal diffusion. A particle diameter larger than the optimum dictates a longer column and thus greater mobile-phase velocity (to maintain the desired void time) and excessive band spreading from resistance to mass transfer. Therefore, there is an optimum particle diameter and a corresponding optimum column length that maximize the resulting column efficiency. For larger analyte molecules with smaller diffusion coefficients, analogous families of curves exist, wherein smaller particle diameters are the optima.

3. EARLY STUDIES: ULTRAHIGH-PRESSURE LIQUID CHROMATOGRAPHY WITH NONPOROUS PACKING MATERIALS

Initial experimental work on UHPLC involved the use of 1.5- and 1.0- μm nonporous silica microspheres [prepared via the Stöber synthesis (8)] bonded with an octadecyl stationary phase (7, 9–14). Although the nonporous nature of these particles results in limited sample-loading capacity, the particles are inherently monodisperse in size, which precludes difficulties associated with classifying a highly disperse mixture of particles into a narrow size cut useful for packing an efficient chromatography column. These nonporous silica particles have been a good reference material with which to study column packing and investigate the feasibility of UHPLC in capillary columns (9–11, 14, 15). **Figure 3a** shows an electron micrograph of some of these particles after they have been extruded from a capillary column with application of modest pressure. **Figure 3b** shows an end view of a fractured column with packing material in place. The side view illustrates the extraordinary consistency in the size of the particles and their tendency to pack into crystalline-like arrays. Crystal defects, such as vacancies and dislocations, are also visible. The end view shows that the ordered structure apparently exists only in the outermost regions of the column, where the particles pack up against the flat surface of the column wall. Away from the column wall, the packing is disordered.

Figure 4 presents example chromatograms of standard test analytes run on a 10- μm -i.d. (inner diameter), 43-cm-long column packed with 1.0- μm nonporous particles. The applied pressure in **Figure 4a** was 3000 bar, near the optimum velocity for these analytes on this column. The image in **Figure 4b** was obtained by increasing the pressure to 7000 bar, resulting in a fast separation but little increase in peak widths. The latter separation was obtained at the highest pressure ever reported for a chromatogram (11).

Column efficiency is influenced dramatically by the i.d. of the capillary tubing used to prepare the column. Shown in **Figure 5** are van Deemter plots for the test analyte hydroquinone for columns of different diameters packed with 1.0- μm nonporous reversed-phase particles (11). There is a regular trend: Performance improves as column diameter decreases. **Figure 6**

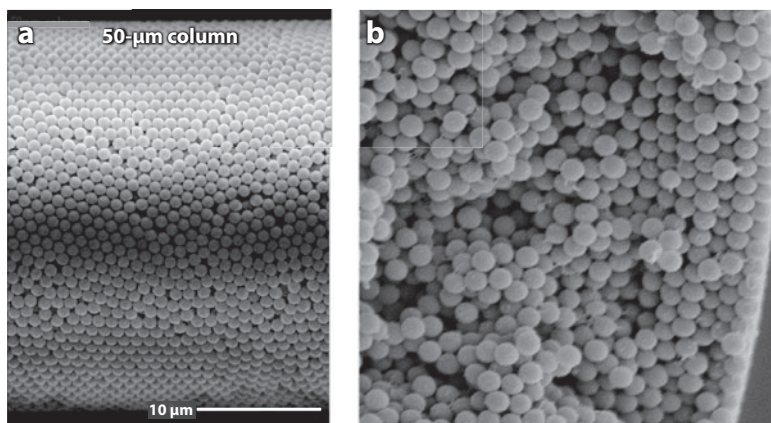


Figure 3

(a) Electron micrograph of an extruded section of a 50- μm -i.d. (inner diameter) column packed with 1- μm nonporous particles. (b) Electron micrograph of the end of a 150- μm -i.d. column packed with 1- μm nonporous particles. The column wall is at the far right side of the image (12).

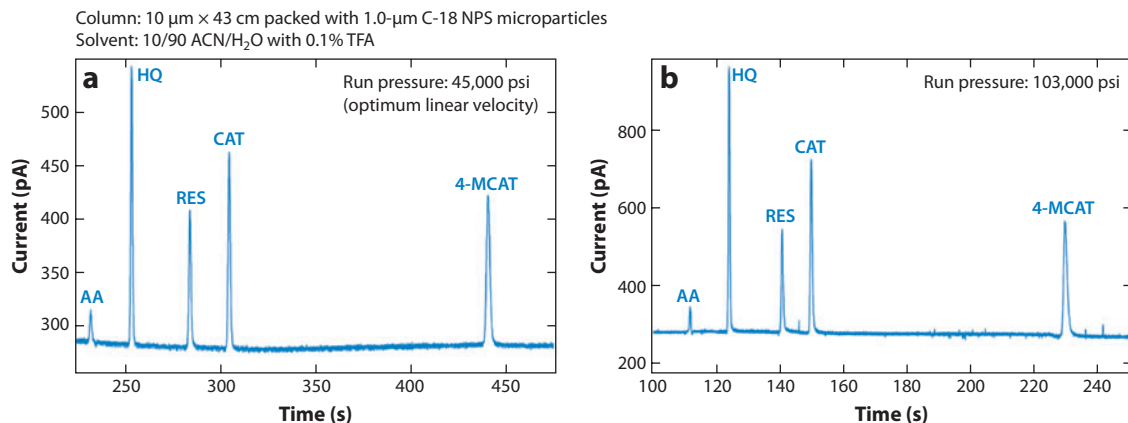


Figure 4

Chromatograms of ascorbic acid (AA), hydroquinone (HA), resorcinol (RES), catechol (CAT), and 4-methylcatechol (4-MCAT) run on a 43-cm-long, 10- μm -i.d. (inner diameter) column packed with 1- μm , nonporous, reversed-phase packing. (a) Pressure: 3000 bar. (b) Pressure: 7000 bar (12).

shows plots of the van Deemter A, B, and C terms for hydroquinone and resorcinol as a function of column diameter. The A term decreases roughly in proportion with the decrease in column diameter, approaching values near zero at the smallest column diameters. The B term, as expected, is fairly independent of column diameter. Like the A term, the C term is strongly dependent on column diameter, decreasing dramatically at the smallest column diameters. Similar trends have been observed in studies of capillary columns packed with larger particles (16–18). Improvement in the A term as column diameter decreases is a result of analyte molecules efficiently sampling, and thus averaging, the various possible flow paths by transcolumn

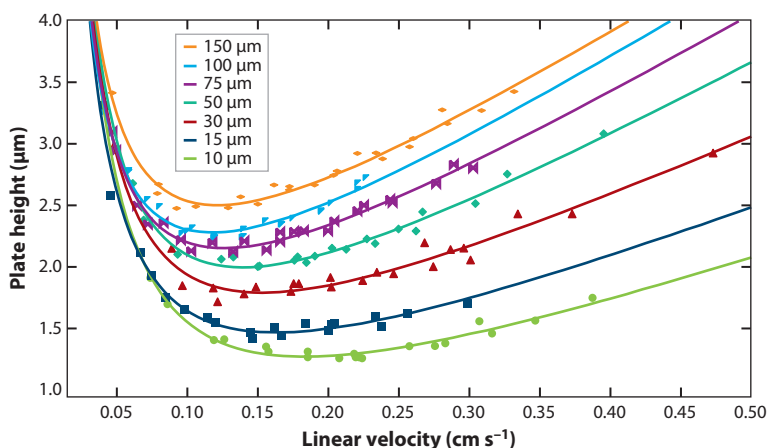


Figure 5

van Deemter plots for hydroquinone, run on columns with diameters ranging from 10 to 150 μm , packed with 1- μm nonporous reversed-phase particles. Lines are a nonlinear least-squares best fit to the van Deemter equation for the data for each column diameter (13).

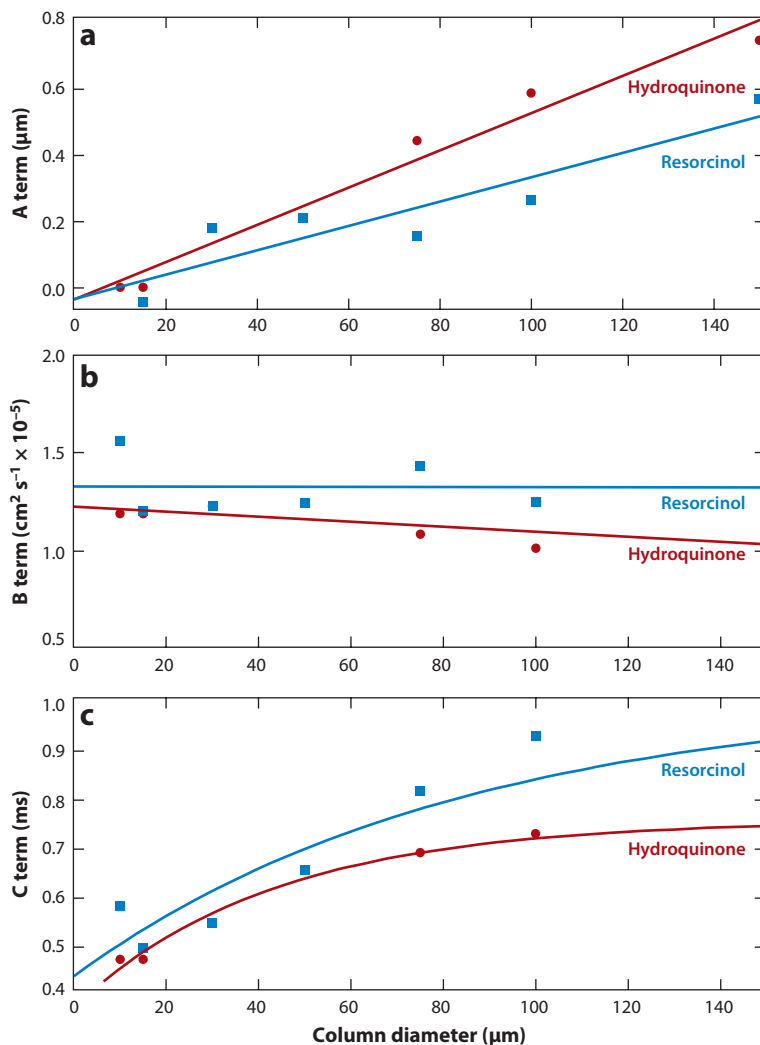


Figure 6

(a–c) Reduced-parameter A, B, and C terms of the van Deemter equation for hydroquinone and resorcinol as a function of column diameter. Data are from the van Deemter curves shown in **Figure 5** (13).

diffusion. The cause of the improvement in the C term with decreasing column diameter is not known.

Pressure effects on retention in HPLC are typically considered relatively insignificant. However, studies carried out by McGuffin and colleagues (19–22), using pressures typical of HPLC conditions, showed significant effects of pressure on retention (10% to 25% change in capacity factor over a pressure range of 100 to 350 bar). These results are of concern for UHPLC conditions, as they extrapolate to greater-than-fivefold changes in capacity factor over the 7000-bar pressure range in UHPLC. If such large changes in capacity factor were to occur, they might confound the analyst. **Figure 7** plots the capacity factors, k' , of a series of test analytes as a function of the column inlet pressure, ranging from atmospheric pressure to more than 4000 bar. In this

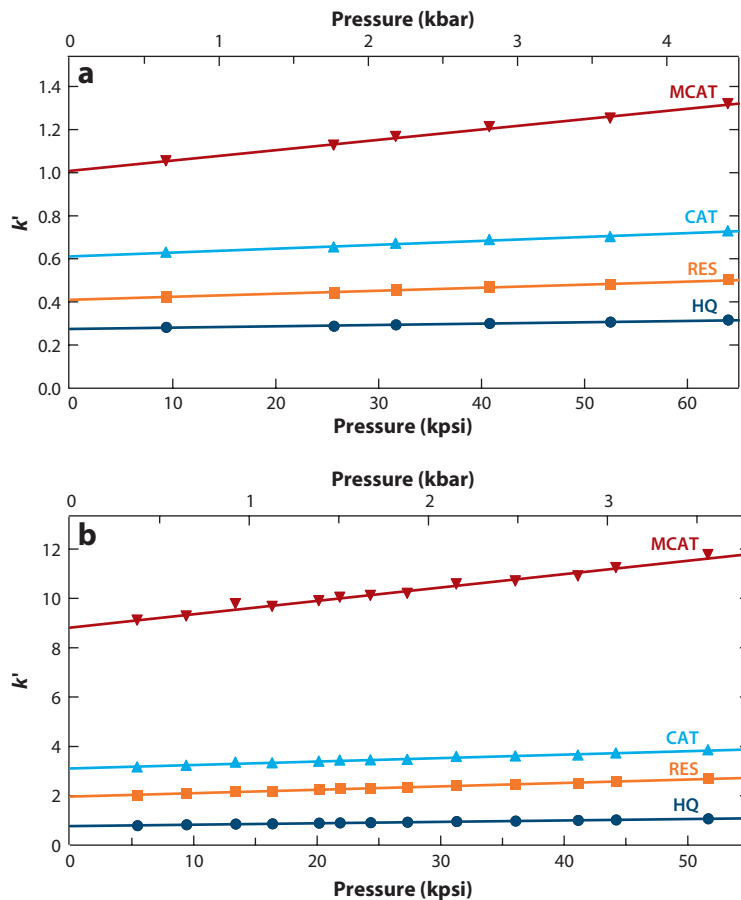


Figure 7

Capacity factors for hydroquinone (HQ), resorcinol (RES), catechol (CAT), and 4-methylcatechol (MCAT) as a function of column inlet pressure. (a) 35/65 volume to volume (v/v) acetonitrile/water. (b) 10/90 v/v acetonitrile/water (23).

instance, the capacity factor is defined as

$$k' = \frac{t_r - t_m}{t_m}, \quad (9)$$

where t_r is the retention time of the test analyte and t_m is the void time of the column (retention time of an unretained marker substance). The data in **Figure 7a** were obtained in 35/65 volume-to-volume (v/v) acetonitrile/water, and the data in **Figure 7b** are in 10/90 v/v acetonitrile/water. There is a modest linear increase in capacity factor with increasing column head pressure, and no extreme changes were observed in this test system (7, 9, 10, 23).

In general, columns packed with silica-based, nonporous, reversed-phase packings measuring 1.0 and 1.5 μm in diameter demonstrated a performance, as judged by their van Deemter curves, that accorded well with expectations from chromatographic theory. Minimum plate heights below two particle diameters were generally obtained.

4. ULTRAHIGH-PRESSURE LIQUID CHROMATOGRAPHY HARDWARE

4.1. Ultrahigh-Pressure Liquid Chromatography Columns

Capillary columns suitable for use in UHPLC are not commercially available. They must be prepared via specialized equipment and techniques.

4.1.1. Column tubing and fritting. The tubing material of choice for preparing capillary UHPLC columns is fused silica, which exhibits ideal properties for a column material. It is flexible, ultraviolet transparent, and very strong. The tensile strength of fused silica is believed to exceed 48,000 bar (24). Fused silica does suffer from the traditional weakness of glasses and ceramics: It is brittle and prone to fracture. This drawback requires that the fused silica be coated with a protective polyimide layer to prevent scratching, which can seriously weaken the tubing.

Before a fused-silica tube can be slurry packed with fine particles, a porous frit must be created in one end of the column. There are a variety of methods to create such frits. A millimeter length of 2.5- μm silica beads can be sintered in the end of the capillary through use of an electric arc heater (9, 25). This method produces a reliable frit that can withstand high pressures and flow shears, but the sintering process removes a short section of polyimide at the capillary end, making this section fragile. An alternative method of column fritting involves a procedure involving Kasil[®] (potassium silicate) and formamide (26). Such frits are prepared at much lower temperatures and thus do not remove the polyimide, but they are less robust than sintered frits and therefore are less likely to survive as an outlet frit during the high-pressure packing process. They are more suitable for use as inlet frits in UHPLC, where they are subjected to much lower stresses and act to prevent particles from escaping from the inlet end of the column during column depressurization.

4.1.2. Column-packing procedure. Capillary columns must be slurry packed at ultrahigh pressures. Particles are slurried in a solvent that ideally reduces particle agglomeration to a minimum. Solvents such as acetone (27), tetrahydrofuran, 30/70 v/v acetone/hexane (9, 10), and even supercritical carbon dioxide (28, 29) have been effective for packing reversed-phase UHPLC packings. The particles must initially be packed at modest pressures so as not to rupture the outlet frit of the capillary column. Packing pressure is usually increased as packing proceeds in order to maintain a relatively steady rate of packing.

The transparency of the fused-silica capillary is an enormous advantage during the packing process because packing can be directly observed via an optical microscope. It is not uncommon for the slurry to cease packing during the process. Blockage of the capillary inlet by an aggregate of particles is suspected to be the cause. Releasing the packing pressure and then reapplying it usually restarts the packing process. The time required to complete the slurry-packing process depends on many variables, including column length, slurry concentration, and solvent viscosity, but times from a few hours to a day are typical.

Once the column is filled to the desired length with slurry, the column is slowly depressurized and an inlet frit is prepared. These steps can be accomplished by a variety of procedures. One procedure is to trim the column to the desired length, then completely dry out the inlet end of the column by allowing the solvent to evaporate. Larger silica particles are then tamped into the end of the column and sintered into place via the electric arcing device for preparing outlet frits (described above) (25). Alternatively, a Kasil/formamide frit can be prepared (26).

4.1.3. Porous packing materials. Nonporous packings are monodisperse in size and are available in sizes that are useful for UHPLC columns. These packings, however, suffer from a lack

of surface area and therefore have a significantly reduced sample-loading capacity compared with porous packing materials. This disadvantage renders nonporous particles impractical for most applications. Porous packings tend to vary widely in size following synthesis, and they require size classification prior to use in packing UHPLC columns. Preparative-level size classification is difficult to perform for particles in the 1- μm range due to their strong tendency to agglomerate. Small quantities of 1.5- and 1.0- μm porous particles, produced by researchers at Waters Corporation, permit one to use them to assess column packing and performance. The 1.5- μm particles, packed using acetone as a slurry solvent, have produced columns that meet the expectations of chromatographic theory (27, 30). Our results from packing columns with 1.0- μm porous particles, however, have been highly variable to date. The columns tend to perform marginally better than do columns packed with 1.5- μm particles. van Deemter analysis of these 1- μm packings shows that an elevated resistance to mass transfer (C term) is largely responsible for the inferior performance (31). Wirth (32) has suggested that slow desorption kinetics from the stationary phase may be the cause of poorer-than-expected performance. The highly variable column-to-column results, according to slurry solvent and column i.d., suggest that the actual physical packing process is at fault and that we have much to learn about the optimum means of packing these 1- μm porous particles. This conclusion is further supported by our observation (31) that extremely small-bore columns (10 μm i.d.) packed with such 1- μm porous particles yield outstanding separation performance with the van Deemter minima of 1.6 particle diameters.

4.2. Mobile-Phase Pumping Systems

Pumps designed for use in UHPLC are not commercially available. They must be adapted from existing high-pressure pumps, which were designed for applications other than LC.

4.2.1. Isocratic pumping. A pneumatic amplifier pump is an inexpensive and simple device for isocratic operation at ultrahigh pressures. Such pumps are available with pressure ratings to 10,000 bar. They function by transferring the force applied by gas pressure exerted on a large cross-section piston directly to a much smaller cross-section piston, which exerts pressure on a liquid. Typical gas/liquid piston-area ratios are 1000 to 1, so a gas pressure of 5 bar translates to a liquid pressure of 5000 bar. Such pumps are constant-pressure rather than constant-flow pumps, but if the column provides a constant flow resistance, a constant flow is achieved. These pumps are suitable for slurry-packing columns, isocratic performance-testing of columns, and routine isocratic operation.

4.2.2. Ultrahigh-pressure liquid chromatography gradient-elution pumping system. An ultrahigh-pressure syringe pump for UHPLC operation has been described (10). This pump was capable of constant flow at pressures as high as 5000 bar, and the flow rate could be computer controlled. The principal reason for the development of this pump was to operate a pair of pumps in tandem to produce binary mobile-phase gradients. This system demonstrated the potential of gradient UHPLC separations, but it was bulky, inconvenient, and generally not amenable to autosampling, rendering it unfit for routine use.

An automated gradient system built around conventional HPLC pumps and hydraulic amplifier pumps was designed and constructed by Keith Fadgen and Geoff Gerhardt of Waters Corporation, and its operation was described by Eschelbach & Jorgenson (33). A schematic of the system and its operation is shown in **Figure 8**. The system generates a mobile-phase gradient at low pressure via a commercial capillary LC system (the CapLC[®]) and stores this gradient in reverse order in a stainless-steel capillary gradient storage tube. Following loading of the gradient, the autosampler

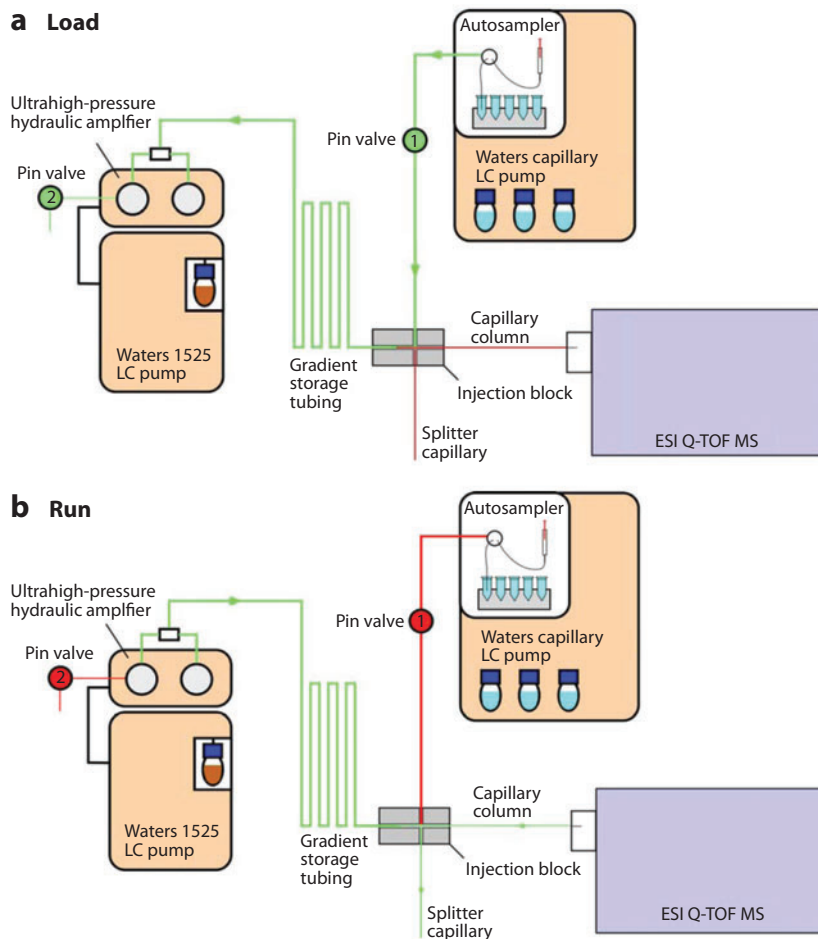


Figure 8

Schematic diagram of gradient pumping system with autosampler. (a) Mobile phase is loaded by the CapLC[®] pump in reverse order (high organic content to low organic content) into the gradient storage tubing. Sample is then loaded into this tubing. The two pin valves are in the open position, allowing fluid to flow from the CapLC into the storage tubing and back through the hydraulic amplifier pump to waste. The very high flow resistance of the capillary column and splitter capillary prevents any significant flow into these two arms of the injection block. (b) The two pin valves are closed, sealing off the waste port on the hydraulic amplifier pump and isolating the CapLC. The Waters 1525 LC pumps hydraulic fluid as a working fluid into the low-pressure side of the hydraulic amplifier pump. Water in the high-pressure side of the hydraulic amplifier pump pressurizes the fluid filling the gradient storage tubing, forcing sample and mobile phase into the injection block. The flow of sample and mobile phase is split in the injection block, and the majority goes to waste through the splitter capillary (43). Abbreviations: ESI Q-TOF MS, electrospray ionization quadrupole time-of-flight mass spectrometry; LC, liquid chromatography.

on the capillary LC loads sample into the same gradient storage tube. Electronically actuated pin valves are then used to isolate the CapLC system. The far end of the gradient storage tube is connected to a hydraulic amplifier pump. This pump works by the same principle as a pneumatic amplifier pump does, except that force from a pressure exerted by a hydraulic fluid pumped at hundreds of bar is applied to a smaller cross-section piston that exerts pressure on the mobile

phase. A conventional HPLC pump is used to apply a constant flow rate on the hydraulic fluid, which translates into a much lower constant flow rate at a much higher pressure applied to the fluid in the gradient storage tube. Completely automated operation is thereby achieved at pressures up to 3000 bar, which is the limit of the pin valves and pumping hardware.

4.3. Sample-Introduction Valves

Loop-injection valves are the standard sample-introduction devices in HPLC. Injection valves usually employ a rotor sliding within a surrounding stator. The rotor provides vias that align with the ports on the surrounding stator. High-strength polymers provide a leak-free seal between the rotor and stator. The difficulty in UHPLC is creating a sample-introduction system that can function at pressures of 3000 bar and higher. A static split-injection system, shown in **Figure 9**, was the first sample-introduction system used in isocratic UHPLC (9). Prior to making an injection, flow from the pneumatic amplifier pump is shut off. The injection valve and waste valve are opened, and sample is introduced by hand from a syringe into the central passage of the injection block, where the capillary column inlet also resides. Once sample has been introduced into the injector block, the injection valve and waste valve are closed. Reduced pressure from the pump (a few hundred bar) is then applied, forcing a small amount of sample to flow into the UHPLC capillary column. After a few seconds, the waste valve is opened and remaining sample is flushed from

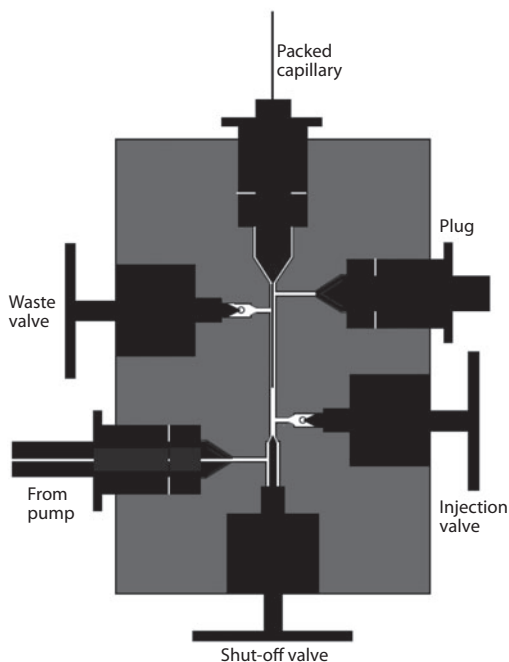


Figure 9

Schematic diagram of a static split-sample injector. Sample loading is accomplished by closing the shut-off valve, opening the injection and waste valves, and loading sample by syringe into the injector. The injection and waste valves are then closed, the shut-off valve is opened, and modest pressure is applied for a few seconds to inject sample into the capillary column. The waste valve is then opened, allowing remaining sample to be flushed from the injector. The waste valve is then closed, and pressure is increased to full run pressure (7).

the injection block. The waste valve is then closed, and full run pressure is applied, initiating the chromatographic separation. This device wastes sample, but it can accomplish a sharp injection. It is useful for column testing and demonstrating the feasibility of UHPLC, but it is not a very practical system, nor is it easily automated. Wu et al. (28) described the operation of an alternative sample valve that utilizes a dynamic splitting system at pressures up to 1200 bar.

Both Anspach et al. (34) and Xiang et al. (35) described operation of an injection loop-type system based upon six pneumatically actuated pin valves. This design eliminates the sliding surfaces of the rotor/stator pair with their large contact area, as in conventional HPLC loop injectors. The system is rated to withstand pressures up to 3000 bar and was operated to pressures of nearly 2000 bar. Very sharp injection profiles were demonstrated, and the system also appears amenable to automation. Its main drawback is that it is a rather bulky and expensive device.

Another sample-introduction system was developed for use with the gradient-elution UHPLC system described by Eschelbach & Jorgenson (33). This approach, shown in **Figure 8**, uses a dynamic split of the sample between the UHPLC capillary column and a splitter capillary, with a few percent of the sample going to the UHPLC column and the remainder going to waste through the splitter capillary. This system can also be operated in a splitless mode, where the splitter capillary is blocked and the entire flow is forced into the analytical column. This splitless mode is only applicable with gradient elution and retained analytes because the long duration of the splitless injection process depends on sample being concentrated on the head of the analytical column and then released by gradient elution. After sample introduction is complete, the splitter capillary is opened, and mobile-phase gradient flow is split between the analytical column and splitter. This system is comparatively simple and readily amenable to automation, but it works best with gradient elution.

5. EXAMPLE SEPARATIONS BY ULTRAHIGH-PRESSURE LIQUID CHROMATOGRAPHY

UHPLC has been used for the separation of a variety of small-molecule entities (36–40) as well as enantiomers (41). It has also been used for the separation of peptides and proteins (10, 33, 42–47). **Figures 10** and **11** show examples of separations of complex mixtures made possible by using UHPLC in a slow gradient-elution mode. **Figure 10** shows a separation of fluorescently labeled peptides from a tryptic digest of hen egg ovalbumin (12). **Figure 11** shows a separation with mass spectrometric detection of the soluble cytosolic proteins from *Escherichia coli*. In both cases, the peaks are remarkably sharp and symmetric. Peak capacities in UHPLC are comparable to those observed in capillary GC and have been demonstrated as high as 1500, permitting the analysis of exceedingly complex mixtures (48).

6. FUTURE ISSUES

6.1. Alternative Retention Modes and Stationary Phases

The vast majority of capillary UHPLC separations have been carried out in reversed-phase mode. Although reversed phase is undoubtedly the most useful LC mode, alternative modes such as ion exchange (49), size exclusion, and normal phase deserve to be studied in a UHPLC setting. All of these modes would benefit from increased plate counts and resolution. Size exclusion in particular may be problematic in a UHPLC format. Size-exclusion packing materials tend to have a high specific pore volume (internal pore volume per gram of packing material) so that they can provide as much volume as possible for retention of solutes. This property tends to make size-exclusion

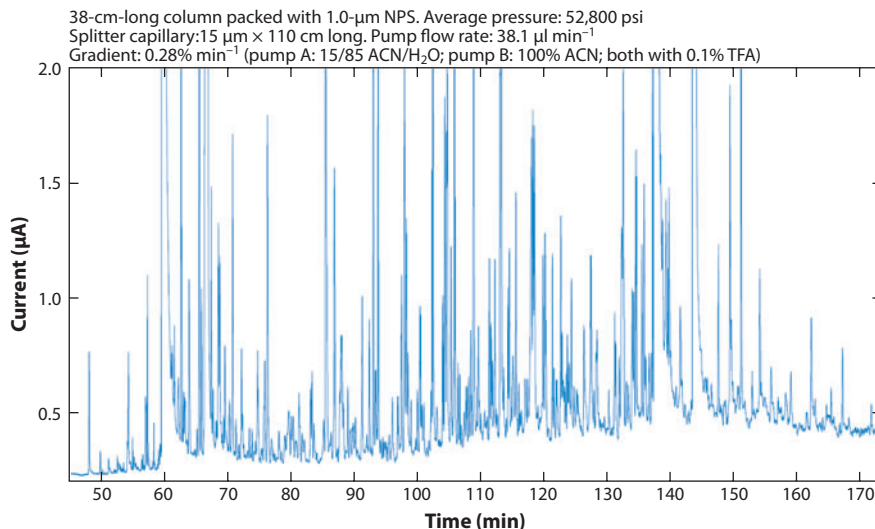


Figure 10

Chromatogram of a tryptic digest of ovalbumin labeled with tetramethylrhodamine isothiocyanate. Columns are 38 cm long and 15 μm i.d. and are packed with 1- μm nonporous reversed-phase particles. Mobile-phase gradient is 15% to 100% acetonitrile at 0.28% min^{-1} . Average run pressure is 3650 bar. The peak capacity in this chromatogram was calculated to be 417, more than double the peak capacity that would be observed in conventional reversed-phase high-pressure liquid chromatography of peptides (12).

packing materials exceptionally fragile, as the volume of solid material is traded away for increased pore volume. This fragility does not bode well for application at the high stress of operation under UHPLC conditions.

6.2. Submicrometer Particles and Superficially Porous Particles

Particles smaller than 1 μm are of particular interest for the separation of analytes of higher molecular weight, such as peptides and proteins. Packing columns with such small particles is challenging due to (*a*) the tendency of these particles to agglomerate and (*b*) the extremely high flow resistance of the resulting columns. Cintron & Colon (15) have described packing columns with 0.67- μm nonporous particles. Due to the high optimum mobile-phase velocity and the high flow resistance of the column, the resulting van Deemter curves were dominated by longitudinal diffusion, and it was impossible for the authors to explore flow regimes where resistance to mass transfer dominated column performance.

Superficially porous particles are an alternative to totally porous particles. They are prepared by growing a porous layer onto monodisperse solid-core particles. Such particles are a hybrid between nonporous particles and totally porous particles, and they retain to a good degree the inherently narrow size distribution of the core particles while also maintaining a majority of the surface area and thus sample capacity of porous particles. Destefano et al. (50) have shown that the performance of 2.7- μm superficially porous particles is on a par with that of sub-2- μm porous particles. The authors explain that the 2.7- μm superficially porous particles can be operated at ordinary HPLC pressures, whereas the sub-2- μm particles require pressures above those of HPLC systems. Use of yet smaller superficially porous particles operated at UHPLC pressures may offer additional possibilities. A 1- μm core with a 0.1- μm porous layer would offer a monodisperse

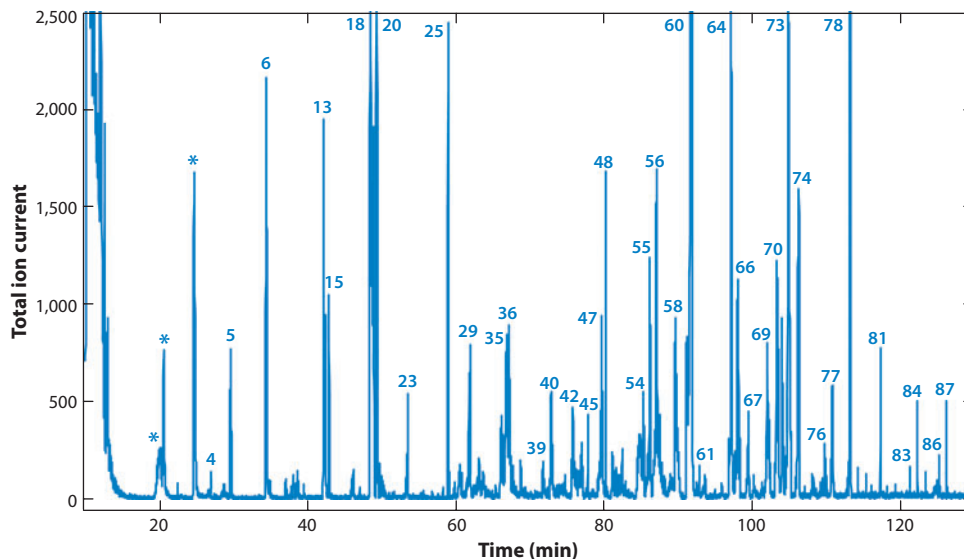


Figure 11

Chromatogram of soluble cytosolic proteins from *Escherichia coli*. Column is 42 cm long by 50 μm i.d. and is packed with 1.5- μm porous reversed-phase particles. Mobile-phase gradient is 25% to 60% acetonitrile at 0.25% min^{-1} . Average run pressure is 1700 bar. All numbered peaks were deconvoluted to yield distinct molecular weights appropriate for proteins. This separation of proteins is significantly superior to separations obtained by conventional high-pressure liquid chromatography (HPLC). Average peak width is 15 s; total peak capacity is 470. This peak capacity is far greater than that observed in reversed-phase HPLC of proteins.

particle measuring 1.2 μm in diameter and would retain almost half of the surface area of a totally porous particle of identical diameter.

Operation of UHPLC columns at higher temperatures is also an attractive possibility (51–53). Increased temperatures provide the benefit of reduced solvent viscosity and increased solute diffusivity, both of which act to permit operation at increased speed.

6.3. Monolith Columns

Monolith columns, which are continuous porous columns synthesized in situ within a surrounding column tube, are an appealing alternative to traditional packed columns. They are prepared by polymerizing either organic monomers or silane monomers. Monoliths feature large macropores, which permit flow through the monolith, and smaller mesopores, which provide surface area for the stationary phase (54–57). Whereas the interparticle porosity of traditional packed columns is fixed at approximately 0.4 by the nature of random packing of particles, monoliths can be designed in a wide range of pore sizes, pore volumes, and overall porosity. The result of this freedom is the ability to prepare columns with equivalent separation power to traditional packed columns but with much greater permeability and thus lower pressure requirements. It is possible, for example, to prepare a monolith column with separating power equivalent to that of 2.5- μm particles but with flow resistance equivalent to that of 5- μm particles (58). The potential disadvantages of monoliths are tied to the fact that preparation of each monolith column is a unique synthesis, both in terms of monolith preparation and in terms of any subsequent bonding of the stationary phase. These

disadvantages may negatively influence the column-to-column reproducibility of these columns. Packing materials for traditionally packed columns can be synthesized and bonded in large batch quantities, thus ensuring a greater likelihood of reproducibility between columns. In the future, it may be desirable to use monolith columns in conjunction with ultrahigh-pressure operation. In so doing, it may be possible to make columns whose flow resistance is equivalent to that of a column packed with 1- μm particles but whose separation power is equivalent that of 0.5- μm particles. The combination of ultrahigh pressures and monolith format would open exciting new vistas in separation power.

6.4. Open Tubular Columns

Open tubular columns offer the greatest potential for extremely high separation efficiency in LC (59–76), but they suffer from a significant disadvantage. The appropriate column diameter in LC is below 5 μm , which necessitates the use of very sensitive detectors. As mass spectrometers continue to improve in terms of speed and sensitivity, open tubular columns may become a more realistic option for LC.

6.5. Physicochemical Data at Ultrahigh Pressure

Although at ordinary HPLC pressures mobile phases may be regarded as relatively incompressible, this is not true at the pressures encountered in UHPLC. There are scarce basic physicochemical data on the effects of ultrahigh pressures on such properties as solvent viscosity (77), solvent compressibility, and solute-diffusion coefficients (78), as well as on the heating effects of solvent compression and expansion (79). Also, although limited data are available for some pure solvents, they are rarely available for the mixed aqueous/organic solvents most commonly used in LC. This is an area in which more fundamental data will be useful.

DISCLOSURE STATEMENT

The author is not aware of any affiliations, memberships, funding, or financial holdings that might be perceived as affecting the objectivity of this review.

ACKNOWLEDGMENTS

I wish to acknowledge the Waters Corporation for its long-term financial and material support of my laboratory's research in UHPLC.

LITERATURE CITED

1. Halász I, Ende R, Asshauer J. 1975. Ultimate limits in high-pressure liquid chromatography. *J. Chromatogr.* 112:37–60
2. Martin M, Eon C, Guiochon G. 1975. Pertinency of pressure in liquid chromatography. III. Practical method for choosing the experimental conditions in liquid chromatography. *J. Chromatogr.* 110:213–32
3. Bidlingmeyer BA, Hooker RP, Lochmuller CH, Rogers LB. 1969. Improved chromatographic resolution from pressure-induced changes in liquid-solid distribution ratios. *Sep. Sci.* 4:439–46
4. Bidlingmeyer BA, Rogers LB. 1972. Pressure-induced changes in the chromatographic selectivity of methyl and ethyl orange on silica gel. *Sep. Sci.* 7:131–58
5. Prukop G, Rogers LB. 1978. Reverse phase ion-pairing chromatography at pressures up to 345 MPa. *Sep. Sci. Technol.* 13:59–78

6. Prukop G, Rogers LB. 1978. Cation exchange at pressures up to 400 MPa. *Sep. Sci. Technol.* 13:127–35
7. MacNair JE. 1998. Ultra high pressure liquid chromatography. PhD thesis. Chapel Hill: Univ. N.C. Press. 241 pp.
8. Stoeber W, Fink A, Bohn E. 1968. Controlled growth of monodisperse silica spheres in the micron size range. *J. Colloid Interface Sci.* 26:62–69
9. MacNair JE, Lewis KC, Jorgenson JW. 1997. Ultrahigh-pressure reversed-phase liquid chromatography in packed capillary columns. *Anal. Chem.* 69:983–89
10. MacNair JE, Patel KD, Jorgenson JW. 1999. Ultrahigh-pressure reversed-phase capillary liquid chromatography: isocratic and gradient elution using columns packed with 1.0-mm particles. *Anal. Chem.* 71:700–8
11. Patel KD, Jerkovich AD, Link JC, Jorgenson JW. 2004. In-depth characterization of slurry packed capillary columns with 1.0-mm nonporous particles using reversed-phase isocratic ultrahigh-pressure liquid chromatography. *Anal. Chem.* 76:5777–86
12. Patel KD. 2001. *Continued studies in ultra high pressure liquid chromatography*. PhD thesis. Univ. N.C., Chapel Hill. 249 pp.
13. Jerkovich AD. 2003. *Band broadening in isocratic ultra-high pressure liquid chromatography*. PhD thesis. Univ. N.C., Chapel Hill. 196 pp.
14. Jerkovich AD, Mellors JS, Thompson JW, Jorgenson JW. 2005. Linear velocity surge caused by mobile-phase compression as a source of band broadening in isocratic ultrahigh-pressure liquid chromatography. *Anal. Chem.* 77:6292–99
15. Cintron JM, Colon LA. 2002. Organo-silica nano-particles used in ultrahigh-pressure liquid chromatography. *Analyst* 127:701–4
16. Karlsson KE, Novotny M. 1988. Separation efficiency of slurry-packed liquid chromatography microcolumns with very small inner diameters. *Anal. Chem.* 60:1662–65
17. Kennedy RT, Jorgenson JW. 1989. Preparation and evaluation of packed capillary liquid chromatography columns with inner diameters from 20 to 50 micrometers. *Anal. Chem.* 61:1128–35
18. Hsieh S, Jorgenson JW. 1996. Preparation and evaluation of slurry-packed liquid chromatography microcolumns with inner diameters from 12 to 33 micrometers. *Anal. Chem.* 68:1212–17
19. McGuffin VL, Evans CE. 1991. Influence of pressure on solute retention in liquid chromatography. *J. Microcolumn Sep.* 3:513–20
20. McGuffin VL, Evans CE, Chen S-H. 1993. Direct examination of separation processes in liquid chromatography: effect of temperature and pressure on solute retention. *J. Microcolumn Sep.* 5:3–10
21. McGuffin VL, Chen S-H. 1997. Molar enthalpy and molar volume of methylene and benzene homologues in reversed-phase liquid chromatography. *J. Chromatogr. A* 762:35–46
22. McGuffin VL, Chen S-H. 1997. Theoretical and experimental studies of the effect of pressure on solute retention in liquid chromatography. *Anal. Chem.* 69:930–43
23. Thompson JW. 2006. *Advancing ultrahigh pressure liquid chromatography through extensions of theory and practice*. PhD thesis. Univ. N.C., Chapel Hill. 251 pp.
24. Kurkjian CR, Albarino RV, Krause JT, Vazirani HN, DiMarcello FV, et al. 1976. Strength of 0.04–50-m lengths of coated fused silica fibers. *Appl. Phys. Lett.* 28:588–90
25. Hoyt AM Jr, Beale SC, Larmann JP Jr, Jorgenson JW. 1993. Preparation and evaluation of an online preconcentrator for capillary electrophoresis. *J. Microcolumn Sep.* 5:325–30
26. Maiolica A, Borsotti D, Rappsilber J. 2005. Self-made frits for nanoscale columns in proteomics. *Proteomics* 5:3847–50
27. Mellors JS, Jorgenson JW. 2004. Use of 1.5-mm porous ethyl-bridged hybrid particles as a stationary-phase support for reversed-phase ultrahigh-pressure liquid chromatography. *Anal. Chem.* 76:5441–50
28. Wu N, Lippert JA, Lee ML. 2001. Practical aspects of ultrahigh pressure capillary liquid chromatography. *J. Chromatogr. A* 911:1–12
29. Lippert JA, Xin B, Wu N, Lee ML. 1999. Fast ultrahigh-pressure liquid chromatography: on-column UV and time-of-flight mass spectrometric detection. *J. Microcolumn Sep.* 11:631–43
30. Mellors JS. 2005. *Development and evaluation of new reversed phase packing materials for ultra-high pressure liquid chromatography*. PhD thesis. Univ. N.C., Chapel Hill. 147 pp.

31. Lieberman R. 2009. *Evaluation of micron sized silica based packing material for ultra high pressure capillary liquid chromatography*. PhD thesis. Univ. N.C., Chapel Hill. 182 pp.
32. Wirth MJ. 2007. Mass transport in sub-2-micron high-performance liquid chromatography. *J Chromatogr. A* 1148:128–30
33. Eschelbach JW, Jorgenson JW. 2006. Improved protein recovery in reversed-phase liquid chromatography by the use of ultrahigh pressures. *Anal. Chem.* 78:1697–706
34. Anspach JA, Maloney TD, Brice RW, Colon LA. 2005. Injection valve for ultrahigh-pressure liquid chromatography. *Anal. Chem.* 77:7489–94
35. Xiang Y, Liu Y, Stearns SD, Plistil A, Brisbin MP, Lee ML. 2006. Pseudolinear gradient ultrahigh-pressure liquid chromatography using an injection valve assembly. *Anal. Chem.* 78:858–64
36. Dong MW. 2007. Ultrahigh-pressure LC in pharmaceutical analysis: performance and practical issues. *LCGC N. Am.* 25:656–58, 660–66
37. Klejdus B, Vacek J, Lojkova L, Benesova L, Kuban V. 2008. Ultrahigh-pressure liquid chromatography of isoflavones and phenolic acids on different stationary phases. *J. Chromatogr. A* 1195:52–59
38. Li X, Fekete A, Englmann M, Goetz C, Rothballer M, et al. 2006. Development and application of a method for the analysis of N-acylhomoserine lactones by solid-phase extraction and ultra high pressure liquid chromatography. *J. Chromatogr. A* 1134:186–93
39. Soliev A, Quiming NS, Ohta H, Saito Y, Jinno K. 2007. Separation of ginsenosides at elevated temperature by ultra high pressure liquid chromatography. *J. Liquid Chromatogr. Relat. Technol.* 30:2835–49
40. Wang H, Edom RW, Kumar S, Vincent S, Shen Z. 2007. Separation and quantification of two diastereomers of a drug candidate in rat plasma by ultra-high pressure liquid chromatography/mass spectrometry. *J. Chromatogr. B Anal. Technol. Biomed. Life Sci.* 854:26–34
41. Gong Y, Xiang Y, Yue B, Xue G, Bradshaw JS, et al. 2003. Application of diaza-18-crown-6-capped β -cyclodextrin bonded silica particles as chiral stationary phases for ultrahigh pressure capillary liquid chromatography. *J. Chromatogr. A* 1002:63–70
42. Eschelbach J. 2006. *Early studies in ultrahigh pressure liquid chromatography of intact proteins*. PhD thesis. Univ. N.C., Chapel Hill. 201 pp.
43. Evans CR. 2007. *Multidimensional liquid chromatography coupled to mass spectrometry for the analysis of complex mixtures of proteins*. PhD thesis. Univ. N.C., Chapel Hill. 248 pp.
44. Evans CR, Jorgenson JW. 2008. Ultrahigh pressure multidimensional liquid chromatography. In *Multidimensional Liquid Chromatography: Theory and Applications in Industrial Chemistry and the Life Sciences*, ed. SA Cohen, MR Schure, pp. 177–204. New York: Wiley Intersci.
45. Kim M-S, Choie W-S, Shin YS, Yu M-H, Lee S-W. 2004. Development of ultra-high pressure capillary reverse-phase liquid chromatography/tandem mass spectrometry for high-sensitive and high-throughput proteomics. *Bull. Korean Chem. Soc.* 25:1833–39
46. Monroe ME. 2002. *Development of instrumentation and applications for microcolumn liquid chromatography coupled to time-of-flight mass spectrometry*. PhD thesis. Univ. N.C., Chapel Hill. 278 pp.
47. Motoyama A, Venable JD, Ruse CI, Yates JR III. 2006. Automated ultra-high-pressure multidimensional protein identification technology (UHP-MudPIT) for improved peptide identification of proteomic samples. *Anal. Chem.* 78:5109–18
48. Shen Y, Zhang R, Moore RJ, Kim J, Metz TO, et al. 2005. Automated 20 kpsi RPLC-MS and MS/MS with chromatographic peak capacities of 1000–1500 and capabilities in proteomics and metabolomics. *Anal. Chem.* 77:3090–100
49. Sousa J. 2004. *Synthesis of superficially porous silica supports and the investigation of strong cation exchange in ultra-high pressure liquid chromatography*. PhD thesis. Univ. N.C., Chapel Hill. 159 pp.
50. Destefano JJ, Langlois TJ, Kirkland JJ. 2008. Characteristics of superficially-porous silica particles for fast HPLC: some performance comparisons with sub-2- μ m particles. *J. Chromatogr. Sci.* 46:254–60
51. Xiang Y, Liu Y, Lee ML. 2006. Ultrahigh pressure liquid chromatography using elevated temperature. *J. Chromatogr. A* 1104:198–202
52. Xiang Y, Yan B, McNeff CV, Carr PW, Lee ML. 2003. Synthesis of micron diameter polybutadiene-encapsulated non-porous zirconia particles for ultrahigh pressure liquid chromatography. *J. Chromatogr. A* 1002:71–78

53. Xiang Y, Yan B, Yue B, McNeff CV, Carr PW, Lee ML. 2003. Elevated-temperature ultrahigh-pressure liquid chromatography using very small polybutadiene-coated nonporous zirconia particles. *J. Chromatogr. A* 983:83–89
54. Tanaka N, Kobayashi H, Nakanishi K, Minakuchi H, Ishizuka N. 2001. Monolithic LC columns. *Anal. Chem.* 73:420–29A
55. Eeltink S, Desmet G, Vivo-Truyols G, Rozing GP, Schoenmakers PJ, Kok WT. 2006. Performance limits of monolithic and packed capillary columns in high-performance liquid chromatography and capillary electrochromatography. *J. Chromatogr. A* 1104:256–62
56. Chen H-S, Rejtar T, Andreev V, Moskovets E, Karger BL. 2005. High-speed, high-resolution monolithic capillary LC-MALDI MS using an off-line continuous deposition interface for proteomic analysis. *Anal. Chem.* 77:2323–31
57. Zhang J, Wu S-L, Kim J, Karger BL. 2007. Ultratrace liquid chromatography/mass spectrometry analysis of large peptides with post-translational modifications using narrow-bore poly(styrene-divinylbenzene) monolithic columns and extended range proteomic analysis. *J. Chromatogr. A* 1154:295–307
58. Hara T, Kobayashi H, Ikegami T, Nakanishi K, Tanaka N. 2006. Performance of monolithic silica capillary columns with increased phase ratios and small-sized domains. *Anal. Chem.* 78:7632–42
59. Jorgenson JW, Guthrie EJ. 1983. Liquid chromatography in open-tubular columns. Theory of column optimization with limited pressure and analysis time, and fabrication of chemically bonded reversed-phase columns on etched borosilicate glass capillaries. *J. Chromatogr.* 255:335–48
60. Dluznieski PR, Jorgenson JW. 1988. New method for the preparation of small diameter columns with polymeric stationary phases for open tubular liquid chromatography. *J. High Resolut. Chromatogr. Commun.* 11:332–36
61. Kennedy RT, Oates MD, Cooper BR, Nickerson B, Jorgenson JW. 1989. Microcolumn separations and the analysis of single cells. *Science* 246:57–63
62. St. Claire RL III, Dohmeier DM, Jorgenson JW. 1991. Preparation of reversed phase open tubular liquid chromatographic columns from borosilicate. *J. Microcolumn Sep.* 3:303–9
63. Tock PPH, Stegeman G, Peerboom R, Poppe H, Kraak JC, Unger KK. 1987. The application of porous silica layers in open tubular columns for liquid chromatography. *Chromatographia* 24:617–24
64. Van Berkel O, Poppe H, Kraak JC. 1987. The application of immobilized liquids for open tubular liquid chromatography. *Chromatographia* 24:739–44
65. Tock PPH, Boshoven C, Poppe H, Kraak JC, Unger KK. 1989. Performance of porous silica layers in open-tubular columns for liquid chromatography. *J. Chromatogr.* 477:95–106
66. Eguchi S, Kloosterboer JG, Zegers CPG, Schoenmakers PJ, Tock PPH, et al. 1990. Fabrication of columns for open-tubular liquid chromatography using photopolymerization of acrylates. *J. Chromatogr.* 516:301–12
67. Tock PPH, Duijsters PPE, Kraak JC, Poppe H. 1990. Theoretical optimization of open-tubular columns for liquid chromatography with respect to mass loadability. *J. Chromatogr.* 506:185–200
68. Van Berkel O, Kraak JC, Poppe H. 1990. Preparation of silicone-coated 5–25- μ m I.D. fused-silica capillary columns for open-tubular liquid chromatography. *J. Chromatogr.* 499:345–59
69. Ruan Y, Feenstra G, Kraak JC, Poppe H. 1993. Preparation and evaluation of cross-linked polyacrylate stationary phases for open tubular liquid chromatography. *Chromatographia* 35:597–606
70. Swart R, Kraak JC, Poppe H. 1994. Preparation and evaluation of polyacrylate-coated fused-silica capillaries for reversed-phase open-tubular liquid chromatography. *J. Chromatogr. A* 670:25–38
71. Swart R, Kraak JC, Poppe H. 1995. Highly efficient separations on 5 μ m internal diameter open tubular capillaries coated with thick polyacrylate stationary phases. *Chromatographia* 40:587–93
72. Swart R, Kraak JC, Poppe H. 1995. Performance of an ethoxyethylacrylate stationary phase for open-tubular liquid chromatography. *J. Chromatogr. A* 689:177–87
73. Swart R, Kraak JC, Poppe H. 1997. Recent progress in open tubular liquid chromatography. *Trends Anal. Chem.* 16:332–42
74. Luo Q, Gu Y, Wu S-L, Rejtar T, Karger BL. 2008. Two-dimensional strong cation exchange/porous layer open tubular/mass spectrometry for ultratrace proteomic analysis using a 10 μ m i.d. poly(styrene-divinylbenzene) porous layer open tubular column with an on-line triphasic trapping column. *Electrophoresis* 29:1604–11

75. Luo Q, Rejtar T, Wu S-L, Karger BL. 2009. Hydrophilic interaction 10- μm I.D. porous layer open tubular columns for ultratrace glycan analysis by liquid chromatography-mass spectrometry. *J. Chromatogr. A* 1216:1223–31
76. Luo Q, Yue G, Valaskovic GA, Gu Y, Wu S-L, Karger BL. 2007. On-line 1D and 2D porous layer open tubular/LC-ESI-MS using 10- μm -i.d. poly(styrene-divinylbenzene) columns for ultrasensitive proteomic analysis. *Anal. Chem.* 79:6174–81
77. Thompson JW, Kaiser TJ, Jorgenson JW. 2006. Viscosity measurements of methanol-water and acetonitrile-water mixtures at pressures up to 3500 bar using a novel capillary time-of-flight viscometer. *J. Chromatogr. A* 1134:201–9
78. Kaiser TJ, Thompson JW, Mellors JS, Jorgenson JW. 2009. Capillary-based instrument for the simultaneous measurement of solution viscosity and solute diffusion coefficient at pressures up to 2000 bar and implications for ultrahigh pressure liquid chromatography. *Anal. Chem.* 81:2860–68
79. Gilpin RK, Zhou W. 2008. Ultrahigh-pressure liquid chromatography: fundamental aspects of compression and decompression heating. *J. Chromatogr. Sci.* 46:248–53



Contents

An Editor's View of Analytical Chemistry (the Discipline) <i>Royce W. Murray</i>	1
Integrated Microreactors for Reaction Automation: New Approaches to Reaction Development <i>Jonathan P. McMullen and Klavs F. Jensen</i>	19
Ambient Ionization Mass Spectrometry <i>Min-Zong Huang, Cheng-Hui Yuan, Sy-Chyi Cheng, Yi-Tzu Cho, and Jentaie Shiea</i>	43
Evaluation of DNA/Ligand Interactions by Electrospray Ionization Mass Spectrometry <i>Jennifer S. Brodbelt</i>	67
Analysis of Water in Confined Geometries and at Interfaces <i>Michael D. Fayer and Nancy E. Levinger</i>	89
Single-Molecule DNA Analysis <i>J. William Efcavitch and John F. Thompson</i>	109
Capillary Liquid Chromatography at Ultrahigh Pressures <i>James W. Jorgenson</i>	129
In Situ Optical Studies of Solid-Oxide Fuel Cells <i>Michael B. Pomfret, Jeffrey C. Owrutsky, and Robert A. Walker</i>	151
Cavity-Enhanced Direct Frequency Comb Spectroscopy: Technology and Applications <i>Florian Adler, Michael J. Thorpe, Kevin C. Cossel, and Jun Ye</i>	175
Electrochemical Impedance Spectroscopy <i>Byoung-Yong Chang and Su-Moon Park</i>	207
Electrochemical Aspects of Electrospray and Laser Desorption/Ionization for Mass Spectrometry <i>Mélanie Abonnenc, Liang Qiao, BaoHong Liu, and Hubert H. Girault</i>	231

Adaptive Microsensor Systems <i>Ricardo Gutierrez-Osuna and Andreas Hierlemann</i>	255
Confocal Raman Microscopy of Optical-Trapped Particles in Liquids <i>Daniel P. Cherney and Joel M. Harris</i>	277
Scanning Electrochemical Microscopy in Neuroscience <i>Albert Schulte, Michaela Nebel, and Wolfgang Schubmann</i>	299
Single-Biomolecule Kinetics: The Art of Studying a Single Enzyme <i>Victor I. Claessen, Hans Engelkamp, Peter C.M. Christianen, Jan C. Maan, Roeland J.M. Nolte, Kerstin Blank, and Alan E. Rowan</i>	319
Chiral Separations <i>A.M. Stalcup</i>	341
Gas-Phase Chemistry of Multiply Charged Bioions in Analytical Mass Spectrometry <i>Teng-Yi Huang and Scott A. McLuckey</i>	365
Rotationally Induced Hydrodynamics: Fundamentals and Applications to High-Speed Bioassays <i>Gufeng Wang, Jeremy D. Driskell, April A. Hill, Eric J. Dufek, Robert J. Lipert, and Marc D. Porter</i>	387
Microsystems for the Capture of Low-Abundance Cells <i>Udara Dharmasiri, Makorzata A. Witek, Andre A. Adams, and Steven A. Soper</i>	409
Advances in Mass Spectrometry for Lipidomics <i>Stephen J. Blanksby and Todd W. Mitchell</i>	433
Indexes	
Cumulative Index of Contributing Authors, Volumes 1–3	467
Cumulative Index of Chapter Titles, Volumes 1–3	470

Errata

An online log of corrections to *Annual Review of Analytical Chemistry* articles may be found at <http://arjournals.annualreviews.org/errata/anchem>.